Flow of sand and a variable mass Atwood machine

José Flores
Departamento de Física "J. J. Giambiagi," Universidad de Buenos Aires, Argentina
and Facultad de Ingeniería y Ciencias de la Universidad Favaloro, Buenos Aires, Argentina

Guillermo Solovey
Departamento de Física "J. J. Giambiagi," Universidad de Buenos Aires, Argentina

Salvador Gil[a)]
Departamento de Física "J. J. Giambiagi," Universidad de Buenos Aires, Argentina,
Escuela de Ciencia y Tecnología de la Universidad Nacional de San Martín, Buenos Aires, Argentina,
and Facultad de Ingeniería y Ciencias de la Universidad Favaloro, Buenos Aires, Argentina

We discuss a simple and inexpensive apparatus that lets us measure the instantaneous flow rate of granular media, such as sand, in real time. The measurements allow us to elucidate the phenomenological laws that govern the flow of granular media through an aperture. We use this apparatus to construct a variable mass system and study the motion of an Atwood machine with one weight changing in time in a controlled manner. The study illustrates Newton's second law for variable mass systems and lets us investigate the dependence of the flow rate on acceleration. © *2003 American Association of Physics Teachers.*

I. INTRODUCTION

Although the formal treatment of variable mass systems is discussed in a number of books on mechanics,[1] until recently, there have been relatively few undergraduate level experiments involving a variable mass.[2–6] However, the study of these systems is an interesting challenge for students and enhances their understanding of the laws of dynamics.

The study of variable mass systems goes back to at least the 16th century. At that time Galileo had already designed an ingenious device and may have been one of the first scientists to study variable mass problems.[7]

Granular materials, of which sand is one example, may be defined as a large conglomeration of macroscopic particles. Despite their apparent simplicity, they behave differently than other forms of matter such as solids and fluids.[6,8] An overview of their surprising features and behavior may be found in Ref. 8. Two reasons for the application of granular materials to variable mass systems are that handling sand is easier than handling a fluid and the constant flow rate of sand, a feature we will explore in Sec. II. This property of the flow allows for a simpler interpretation of the experimental results.

Yersel[6] has suggested that the flow rate of a granular material of density ρ, flowing through an opening of area A under the influence of an effective gravitational field g, is given by

$$\frac{dm}{dt} = k\rho g^{1/2} A^{5/4}, \tag{1}$$

where k is a constant. The dependence of the flow rate on the diameter of circular apertures was measured in Ref. 6 and for this geometry the experimental results agree with Eq. (1).

We will study the flow of sand through an opening using a new device that improves and simplifies the static method used in Ref. 6 and is simple to implement in an undergraduate physics laboratory. As we will see, this method lets us measure the flow rate in real time, making it simple to verify if the flux of granular material is constant in time.

Section III is devoted to the experimental study of an Atwood machine with a variable mass. An approximate solution of the equation of motion is found analytically and compared to experimental data. This device also provides us with an accelerated system that lets us investigate the dependence of the flow rate on acceleration.

II. EXPERIMENTAL CHARACTERIZATION OF FLUXES

For liquids, the time rate of the mass discharged through an orifice depends on the height of the column and thus is time dependent. In contrast, we will show that the flow rate of sand is constant in time and does not depend on its height.

To characterize the sand flow rate, we hung a plastic bottle filled with sand upside down. We drilled openings of different sizes and shapes in several lids and used them to study the flow as a function of the size and shape of the opening. The bottle was hung from a force sensor connected to a data acquisition system associated with a computer (see Fig. 1). In this way, the apparatus measures the mass as a function of time. We obtained the mass flow rate from the slope of the straight line fitted to the data.

The experimental arrangement shown in Fig. 1 was also used to study the flow rate of liquids. As can be seen in Fig. 2, the flow rate of water depends, as expected, on the difference in pressure on the two sides of the opening,[9] and is time dependent. For this experiment the sand must be dry, because a sand castle does not flow in the same way as grains of sand in an hourglass. Common sand, previously sifted, was used. Measurements of the grains using a microscope showed the grains to be about 100 μm across.

Figure 3 shows that the flow rate of sand is constant and increases monotonically with the area of the opening. If we plot the constant flow rate, $c \equiv -dm/dt$, for each opening of area A on a logarithmic scale for both variables, the relation between c and A is a straight line (see Fig. 4). Hence, our results indicate that the phenomenological dependence of c on A is given by
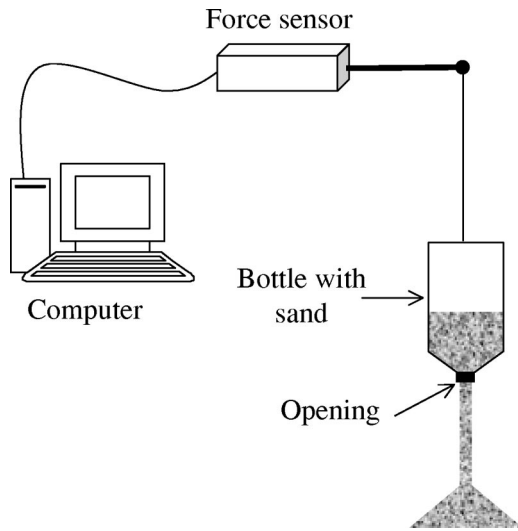
Fig. 1. Schematic of the experimental setup for measuring the flow of sand through different size openings. The bottle is hung from a force sensor that is connected to a data acquisition system associated with a computer. Lids with different size openings are used to study the dependence of the flow rate on the dimensions of the openings.

Fig. 3. The mass as a function of time for circular openings of diameter D. The error in the measurement of the diameters is 0.1 mm. In all cases, the flow of sand is constant.

$$c = bA^v, \qquad (2)$$

where b is a constant that can be obtained from the experimental data. The value of the exponent v was found to be 1.25 ± 0.05. For circular openings, we can write $c \propto D^{2.5}$, where D is the diameter of the circular hole. This result is in agreement with Ref. 6.

Curiosity may have killed the cat, but it drives science, so we wondered how the shape of the opening affects the flow. We took more lids and cut different shaped openings (square and triangular). Not surprisingly, the flow was still constant. What did come as a surprise was that the flow followed the same systematic trend as did the circular openings. From the plot in Fig. 4, we see that the new data points fall on the same functional form as that of the circular holes. This suggests that as long as the characteristic length of the opening is much larger than the size of the grains, the relevant parameter that determines the flux is the area of the opening.

III. AN ATWOOD MACHINE WITH A VARIABLE MASS

Atwood's machine is a textbook example of the application of Newton's second law. A delightful demonstration based on the principles of the Atwood machine is the experiment of the "cup and the key." This experiment is bound to amuse, surprise, and challenge kindergarten children as well as physics professors.[10,11] Take a heavy object such as a cup, attach it to one end of a meter long string, and attach a light object such as a key to the other end of the string. Take a pencil and hold it horizontally with a firm grip. Let the cup hang just below the pencil and drape the string around the pencil. With your other hand, hold the key so that most of the string is horizontal. Can you predict what happens if you release the key?

The Atwood machine consists of two masses, m_1 and m_2, connected by a string running over two identical pulleys that can be regarded as a single pulley of effective mass m_p and radius R_p (see Fig. 5). We slightly changed this configuration by allowing one of the masses to vary with time. This system is interesting because the underlying physics of the system is
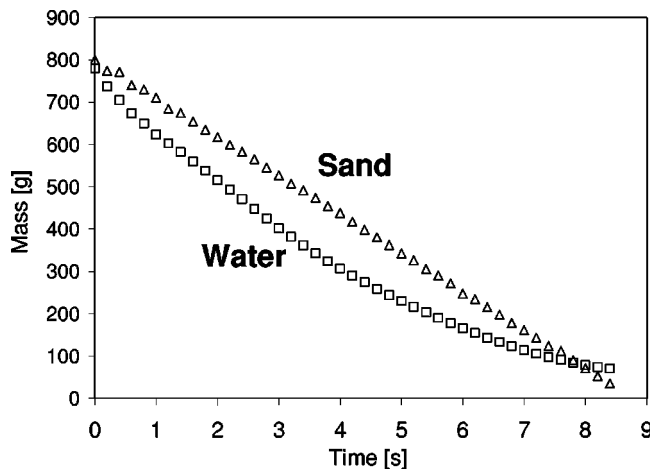

Fig. 2. Comparison of the flow rate of water versus sand. The flow of water, in g/s, clearly decreases with the height of the column, while sand does not.
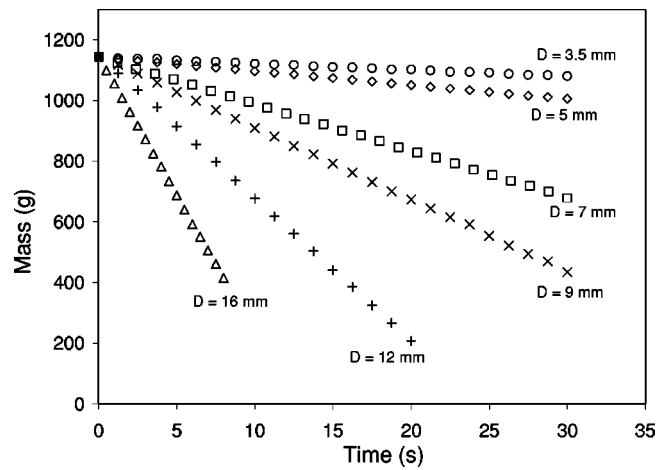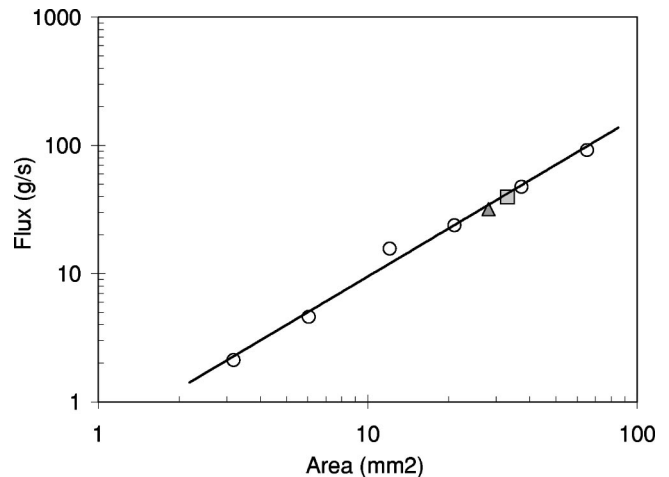

Fig. 4. Relation between the flow and the area of the orifice. The triangular and the square shaped points correspond to similarly shaped openings.
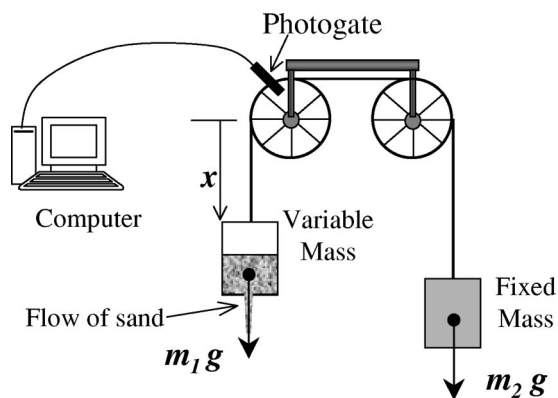
Fig. 5. Schematic of the experimental setup for a variable mass Atwood machine. The photogate, associated with the left pulley, was connected to the computer to collect data. Sand comes from the bottom of the left-hand container.

Fig. 6. Determination of the friction force for the Atwood machine with a constant mass.

transparent and the equations of motion can be solved analytically, making it possible to understand the nature of Newton's second law when applied to variable mass systems.

This arrangement is not new, and the Atwood machine with a changing mass has been studied by several authors.[3–5] Some authors have used a container with water that drips through a hole.[3] Because the flux of water changes in time, the assumption that the flow rate was constant is far from accurate.[3] Other authors have used a container with sand for the variable mass,[4,5] but the functional form for the flow rate was assumed but not independently verified in the same experiment. Moreover, the effects of the friction force and the moment of inertia of the pulleys were disregarded. We have included these effects and tested our assumptions regarding the variation of the flow rate with the acceleration. This approach lets us check the validity of all our assumptions in the same experiment.

Our variable mass system consists of the same inverted plastic bottle filled with sand, and a circular opening in the screw-on lid as was used in the first experiment. We measure the position of one of the masses, $x(t)$, using a smart pulley (a pulley with spokes) and a photogate connected to a computer. The computer provides the time interval between consecutive passes of the spokes. By measuring the diameter of the pulley and the number of spokes, it is straightforward to obtain $x(t)$ and $v(t)$. There is a minor uncertainty in determining the distance traveled by the system at the instant that the pulley reverses direction. This uncertainty produces a kink in the plot of $v(t)$ at this instant.

In principle, it would be possible to obtain the acceleration of the system as well, but, in practice, it is not that simple to differentiate experimental data. Let us assume that we want to determine the velocity v_i from the experimentally measured values of the position x_i and time t_i at two consecutive steps (the subindex i enumerates the sequence of discrete measurements of position and time). Then

$$v_i \cong \frac{x_i - x_{i-1}}{t_i - t_{i-1}}. \tag{3}$$

We suppose that our data has errors σ_x and σ_t for the measurement of position and time, respectively. If we use the conventional procedures for error propagation,[12] we have
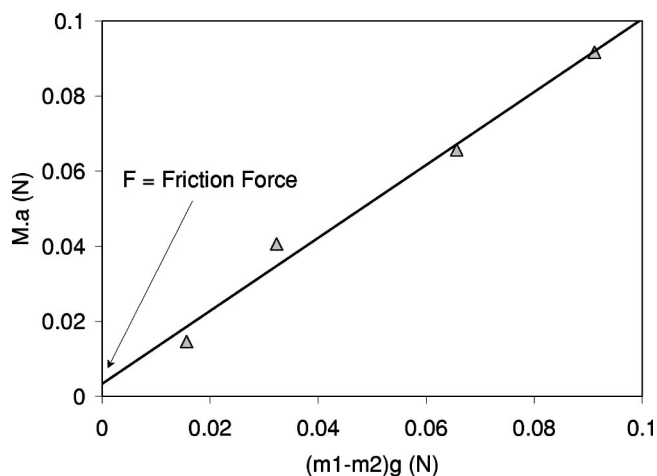
$$\frac{\sigma_v^2}{v_i^2} \approx 2 \frac{\sigma_t^2}{(t_i - t_{i-1})^2} + 2 \frac{\sigma_x^2}{(x_i - x_{i-1})^2}. \tag{4}$$

The uncertainties σ_x and σ_t depend on the quality of our measurements, and for a given experimental setup are approximately constant. Therefore, Eq. (4) indicates that if we take the limit of making the measurement as often as we can, that is, we take $t_i - t_{i-1} \to 0$, the error will dominate our estimate of the derivative. For this reason, it is preferable to compare our model without differentiating the data. Thus, to determine the flow rate, we fitted a straight line through successive time intervals and extracted the slope from the fit to provide an estimate of the derivative.

A. Constant mass

The traditional approach to constant mass systems involves drawing free body diagrams for each part (m_1, m_2, and the pulley).[1,4] We will use a qualitative approach and obtain the same result. The total inertia of the system is made up of the two masses plus a contribution from the pulley. The force that drives the system is the difference in weight between m_1 and m_2. We also consider a constant friction force F due to the pulley opposing the motion. The equation of motion for the system is

$$\left(m_1 + m_2 + \frac{I}{R^2} \right) a = (m_1 - m_2)g - F, \tag{5}$$

where I is the pulley's moment of inertia. If we take $I \cong 0.5 \, m_p R^2$ and define an effective mass $M = m_1 + m_2 + 0.5 \, m_p$, we see that Atwood's machine is analogous to a system of mass M subject to a force $(m_1 - m_2)g - F$. In other words,

$$M \, a = (m_1 - m_2)g - F. \tag{6}$$

By measuring the acceleration for different m_1 and m_2 and plotting Ma as a function of $(m_1 - m_2)$, we obtain a straight line (see Fig. 6), independently verifying the hypothesis that F is constant. From the slope of Fig. 6, we obtain the value of g, which is consistent with the known local acceleration of gravity. The intersection of the fitted line of Fig. 6 with the vertical axis yields $F = (3.3 \pm 0.1) \times 10^{-3}$ N. To extract the acceleration, we plotted the velocity as a function of time by

fitting a straight line through the data. Similarly, it would be possible to plot the position, $x(t)$, versus time and obtain the acceleration by fitting a second-order polynomial. This procedure avoids differentiating the experimental data twice.

B. Discharging mass

Newton's second law for one-dimensional motion can be written as

$$\frac{dP}{dt} = F_T, \tag{7}$$

where P is the total momentum of the system and F_T is the net force acting on it. Because the mass of the system varies in time, we must be very careful when we refer to P in Eq. (7), because it includes the momentum of the discharged mass. Let us consider the variation of momentum between t and $t+\Delta t$. At time t the effective mass M of the system is moving with a velocity v, and the momentum is $P = Mv$. After Δt, the system has discharged a mass $\Delta M (<0)$ and its velocity has changed by Δv. If the sand leaves the system with a velocity u relative to the container, the total momentum at $t+\Delta t$ is

$$P(t+\Delta t) = (M+\Delta M)(v+\Delta v) - (v+u)\Delta M. \tag{8}$$

We assume that the initial relative velocity u of the sand leaving the container is zero ($u=0$). The change in the total momentum to first order becomes

$$\Delta P(t) = P(t+\Delta t) - P(t)$$
$$= (M+\Delta M)(v+\Delta v) - v\Delta M - vM. \tag{9}$$

Therefore, in the limit of $\Delta t \rightarrow 0$, we have

$$\frac{dP}{dt} = M(t)\frac{dv}{dt}, \tag{10}$$

which is similar to the expression for the case of constant mass, but with the important difference that the mass $M(t)$ now varies in time. If we allow mass m_1 to change in time, Eq. (6) becomes

$$M(t)a = (m_1(t) - m_2)g - F, \tag{11}$$

with $M(t) = m_1(t) + m_2 + 1/2\,m_p$.

Because the geometry of the experimental setup is the same as that used previously for the case of constant mass, we expect the friction F not to change. We expect the flow rate to change with acceleration. Indeed if the container were in free fall, no sand would leave the system. According to Ref. 6, the flux will vary with the vertical acceleration as

$$c(a) = c_0(1 + a/g)^\alpha, \tag{12}$$

where c is the flux rate ($-dm/dt$) at the acceleration a, and c_0 is the flux when no acceleration is present. The sign convention for the acceleration is such that if the system is in free fall, $a = -g$. The dependence of the flux on acceleration in Eq. (12) shows the expected behavior for $a=0$ and $a=-g$. By dimensional analysis, Ref. 6 concluded that α in Eq. (12) is equal to $\frac{1}{2}$; we will test this conclusion using our data.

If $a \ll g$, we can use the approximation

$$c(a) \approx c_0\left(1 + \alpha\frac{a}{g}\right). \tag{13}$$

We define the parameters

$$m_{1,0} = m_1(t=0), \quad m_{12,0} = m_{1,0} - m_2, \tag{14}$$

and

$$M_0 = M(t=0) = m_{1,0} + m_2 + 1/2m_p, \tag{15}$$

and combine Eqs. (11) and (13):

$$a(t) = \frac{dv}{dt} = \frac{(m_{12,0} - c_0 t)\cdot g - F}{(M_0 - c_0\lambda t)}. \tag{16}$$

We have defined

$$\lambda = \left(1 - \alpha\left(1 - \frac{a}{g}\right)\right). \tag{17}$$

We can see that because λ depends linearly on a, it is not possible to integrate Eq. (16) by simple methods. However, we can approximate a/g in Eq. (17) by its average value calculated using Eq. (11), and replace m_1 by its mean value, $\langle m_1(t)\rangle \approx m_{1,0}/2$, and disregard the friction force. Therefore, using the parameters M_0 and $m_{1,0}$, introduced previously, we obtain

$$\lambda \approx 1 - \alpha\left(1 - \frac{\frac{1}{2}m_{1,0} - m_2}{M_0 - \frac{1}{2}m_{1,0}}\right) = 1 - \alpha\left(\frac{2m_2 + \frac{1}{2}m_p}{M_0 - \frac{1}{2}m_{1,0}}\right). \tag{18}$$

Equation (16) can now be integrated analytically yielding an expression for both the velocity and the position of one of the masses:

$$v(t) = v(t=0) + \frac{gt}{\lambda} + \frac{(M_0 - \lambda m_{12,0})\cdot g + \lambda F}{c_0\lambda^2}$$
$$\times \ln\left(1 - \frac{c_0\lambda t}{M_0}\right), \tag{19}$$

$$x(t) = x(t=0) + v(t=0)t + \frac{gt^2}{2\lambda}$$
$$+ M_0\frac{(M_0 - \lambda m_{12,0})g + \lambda F}{c_0^2\lambda^3}\left(1 - \frac{c_0\lambda t}{M_0}\right)$$
$$\times \left[\ln\left(1 - \frac{c_0\lambda t}{M_0}\right) - 1\right]. \tag{20}$$

Equations (19) and (20) can be compared directly with the results of our measurements. From the comparison we can assess the validity of our model and obtain the value of α, the only free parameter.

C. Results

Figures 7 and 8 show examples of measurements from our variable mass experiment compared to the theoretical curves obtained from Eqs. (19) and (20) for different values of α. From this comparison, our experimental results are consistent with the value $\alpha = 0.5$. In fact, with a limit of confidence of 95%, $\alpha = 0.5 \pm 0.1$, which agrees with the prediction of Eq. (1). The uncertainty in α can be reduced by experimenting with an increased output flux at higher accelerations, because at larger fluxes, the predictions of Eqs. (19) and (20) are more sensitive to small variations of the parameter α as Figs. 7 and 8 clearly show. Figures 7 and 8 indicate that our results for $x(t)$ and $v(t)$, given by Eqs. (19) and (20), are in complete agreement with the experimental results, even for values of $a \approx g$.
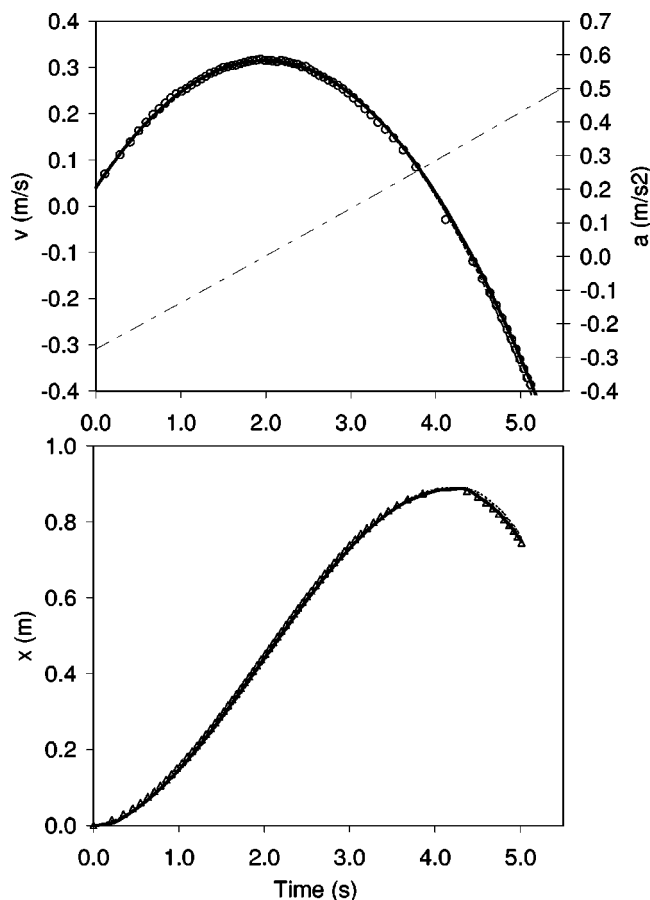
Fig. 7. Experimental result for a small flow rate, $c_0 = 1.7$ g/s. The circles in the upper panel represent the measured values of the velocity as a function of time. The dot-dashed line represents the acceleration obtained using Eq. (16) with $\alpha = \frac{1}{2}$. In the lower panel the triangular symbols represent the measured values of the position as a function of time. In both panels, the heavy continuous line represents the prediction of the model, Eqs. (18) and (19) for $\alpha = 0.5$. The lines corresponding to the prediction of the model for $\alpha = 1$ and $\alpha = 0$ barely differ from the case of $\alpha = 0.5$. The parameters of the system were $m_{10} = 58.9$ g, $m_2 = 55.25$ g, and $m_p = 11$ g.

IV. CONCLUSIONS

We designed a device to measure the flow of sand through an opening. Our measurements show that the flow of sand is constant and depends only on the area of the orifice. The shape of the orifice does not affect the flux as long as the characteristic dimensions of the opening are much larger than the sizes of the grains (see Fig. 4). The experimental results on the dependence of the flow on area agree with the result of a dimensional analysis, that is, the flow depends on the area of the orifice with an exponent of $\frac{5}{4}$ as in Eq. (2).

We also built a variable mass Atwood machine to study the dynamics of a variable mass system. The simplicity of the device allowed us to find good agreement between the theoretical approach and the experimental results. Furthermore, this device has allowed us to explore the dependence of the flow of granular media in an accelerated system, which also gave us insight into how the flow of granular media may change where the acceleration of gravity is different from that on earth. Our results are consistent with the hypothesis that the flow rate of granular media increases proportionally with the square root of the total acceleration of the system.
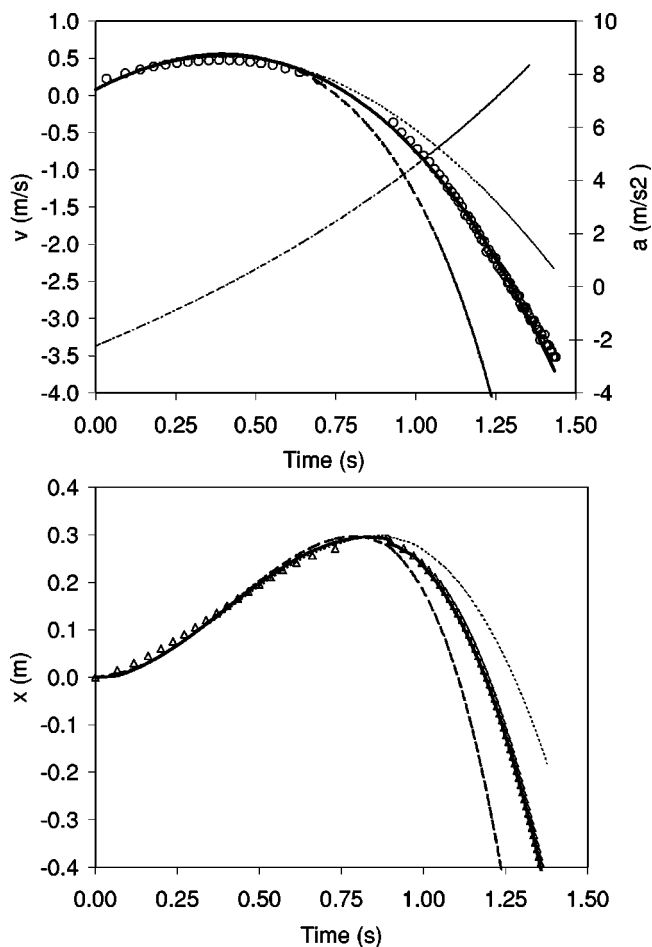

Fig. 8. Experimental result for a large flow rate, $c_0 = 296$ g/s. The circles in the upper panel represent the measured values of velocity as a function of time. The dot-dashed line represents the acceleration obtained using Eq. (16) with $\alpha = \frac{1}{2}$. In the lower panel the triangular symbols represent the measured values of the position as a function of time. In both panels, the heavy continuous line represents the prediction of the model, Eqs. (18) and (19), for $\alpha = 0.5$. The dot-dashed line corresponds to the prediction of the model for $\alpha = 1$. The dashed line corresponds to the prediction of the model for $\alpha = 0$, that is, no dependence of the flow rate with acceleration. The kink observed near the maximum of $x(t)$ is an artifact due to the uncertainty in determining the distance traveled by the system at the instant at which the pulley reverses its direction of motion. The parameters of the system were $m_{10} = 317$ g, $m_2 = 20$ g, and $m_p = 11$ g.

[a]Author to whom correspondence should be addressed. Electronic mail: sgil@df.uba.ar

[1]A. Sommerfeld, *Lectures on Theoretical Physics*, 2nd ed. (Academic, New York, 1964), Vol. I, Chap. I.

[2]K. Y. Shen and Bruce L. Scott, "The hourglass problem," Am. J. Phys. **53** (8), 787–788 (1985).

[3]M. Stautberg Greenwood, R. Bernett, M. Benavides, S. Granger, R. Plass, and S. Walters, "Using a smart-pulley Atwood machine to study rocket motion," Am. J. Phys. **57** (10), 943–946 (1989).

[4]Peter Sullivan and Anna McLoon, "Motion of a sand-filled funnel: An experiment and model," Phys. Teach. **38**, 500–502 (2000).

[5]David Byrd and Gray White, "Alternative theoretical method for motion

of a sand-filled funnel experiment," Phys. Teach. **39** (8), 464–465 (2001).

[6]Metin Yersel, "The flow of sand," Phys. Teach. **38** (5), 290–291 (2000).

[7]P. Bozzi, C. Mccagni, L. Olivieri, and T. B. Settle, *Galileo e la Scienza Sperimentale* (Dipartimento di Física "Galileo Galilei" Universita di Padova, Padova, 1995), p. 51. The "forza della percossa" (force of impact) described in "Giornata sesta dei Discorsi," a modern version of Galileo inquiry, is discussed in Ref. 2.

[8]Heinrich M. Jaeger, Sidney R. Nagel, and Robert P. Behringer, "The physics of granular materials," Phys. Today **49** (4), 32–38 (1996).

[9]D. F. Young, B. R. Munson, and T. H. Okisii, *Fundamentals of Fluid Mechanics*, 2nd ed. (Wiley, New York, 1994), Chap. 9, p. 599.

[10]A. R. Marlow, "A surprising mechanics demonstration," Am. J. Phys. **59** (10), 951–952 (1991).

[11]D. J. Griffiths and T. A. Abbott, "Comments on: 'A surprising mechanics demonstration,' " Am. J. Phys. **60** (10), 951–953 (1992).

[12]S. Gil and E. Rodríguez, *Física re-Creativa* (Prentice Hall, Buenos Aires, 2001), Chap. 17, p. 91, and ⟨www.fisicarecreativa.com⟩.

DEGREES OF FREEDOM

a
pen-
dulum
can only
swing (no
matter how
fast how slow) can
only swing in that
small space (no matter
how fast how slow,
no matter) it can
only swing

one

degree

one

degree

of freedom,

that is what it is
called, that limit cycle,
(back & forth, no matter,
back & forth, fast and slow):
one degree of freedom

But

there is a way
to get more

there is a way
to move

there is a way
to reach
infinite
degrees of
freedom:

move   towards

chaos,   move

towards   change,

move   towards

turbulence

there

are   so

many

degrees

of

freedom

there

so

many

degrees

uncounted

uncountable

a   rolling   ring

of

freedom

so   many

degrees

of

freedom

this   close

to

chaos

Patricia Monaghan, *Dancing with Chaos*
(Salmon Publishing Ldt, Claire, Ireland, 2002).